JACS
JOURNAL OF THE AMERICAN CHEMICAL SOCIETY
pubs.acs.org/JACS
Article

Effects of Glutamate Arginylation on α-Synuclein: Studying an Unusual Post-Translational Modification through Semisynthesis

Buyan Pan, Naoki Kamo, Marie Shimogawa, Yun Huang, Anna Kashina, Elizabeth Rhoades,* and E. James Petersson*

Cite This: J. Am. Chem. Soc. 2020, 142, 21786–21798
Read Online
ACCESS | Metrics & More | Article Recommendations | Supporting Information

ABSTRACT: A variety of post-translational modifications (PTMs) are believed to regulate the behavior and function of α-synuclein (αS), an intrinsically disordered protein that mediates synaptic vesicle trafficking. Fibrils of αS are implicated in neurodegenerative disorders such as Parkinson's disease. In this study, we used chemical synthesis and biophysical techniques to characterize the neuroprotective effects of glutamate arginylation, a hitherto little characterized PTM in αS. We developed semisynthetic routes combining peptide synthesis, unnatural amino acid mutagenesis, and native chemical ligation (NCL) to site-specifically introduce the PTM of interest along with fluorescent probes into αS. We synthesized the arginylated glutamate as a protected amino acid, as well as a novel ligation handle for NCL, in order to generate full-length αS modified at various individual sites or a combination of sites. We assayed the lipid−vesicle binding affinities of arginylated αS using fluorescence correlation spectroscopy (FCS) and found that arginylated αS has the same vesicle affinity compared to control protein, suggesting that this PTM does not alter the native function of αS. On the other hand, we studied the aggregation kinetics of modified αS and found that arginylation at E83, but not E46, slows aggregation and decreases the percentage incorporation of monomer into fibrils in a dose-dependent manner. Arginylation at both sites also resulted in deceleration of fibril formation. Our study represents the first synthetic strategy for incorporating glutamate arginylation into proteins and provides insight into the neuroprotective effect of this unusual PTM.

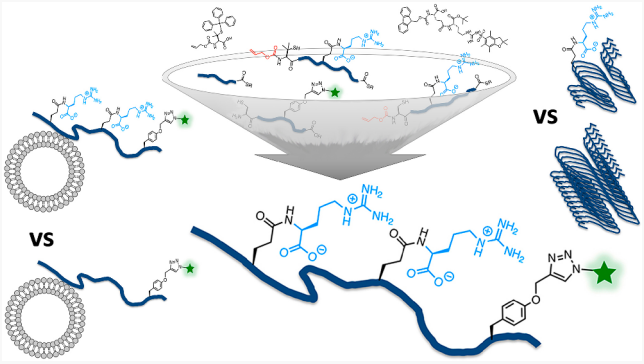

INTRODUCTION

α-Synuclein (αS) is a 14 kDa protein found at the synaptic termini of neurons. An intrinsically disordered protein, it is normally monomeric and does not have a stable, globular fold in solution. The purported native role of αS is to mediate synaptic vesicle fusion, contributing to the relaying of chemical signals between neurons. The abnormal aggregation of αS underlies a class of neurodegenerative diseases known as synucleinopathies. The accumulation of αS in fibrillar deposits known as Lewy bodies is observed in patients with Parkinson's disease.[1]

While the molecular details of αS's native role and pathology have not been fully elucidated, a variety of post-translational modifications (PTMs) have been shown to modulate the structure and function of αS *in vivo*. PTMs are chemical modifications made to proteins after translation, largely through enzymatic processes that give rise to the diversity of forms in which proteins exist and thus the complexity of their behavior. One PTM that was uncharacterized until recently is arginylation, the post-translational transfer of this amino acid onto a protein by Arg-tRNA-protein-transferase (ATE1).[2] Mass spectrometry methods allowed initial identification of arginylation at the N-terminus of a variety of proteins that play critical roles in cardiovascular development and angiogenesis.[3,4] Later, it was found that ATE1 also catalyzes the arginylation of protein side chain carboxylates, including two arginylated glutamate (E^{Arg}, Scheme 1) sites in αS.[5]

In studies to date, arginylation of αS glutamates 46 and 83 has been proposed to serve a neuroprotective role. Notably, αS does not contain any native arginine residues. The occurrence of E^{Arg} has been observed *in vivo* and is thought to reduce αS accumulation in cells, as demonstrated by a resistance to the induction of aggregate formation by preformed αS fibrils in ATE1-expressing neurons.[6] Previously published work by the Kashina laboratory has studied these effects using Ala mutations at arginylation sites Glu46 and Glu83. In these mutant constructs, arginylation has no means to occur (i.e.,

Received: September 20, 2020
Published: December 18, 2020

https://dx.doi.org/10.1021/jacs.0c10054
J. Am. Chem. Soc. 2020, 142, 21786−21798

Scheme 1. Semisynthesis of Arginylated, Fluorescently-Labeled αS[a]

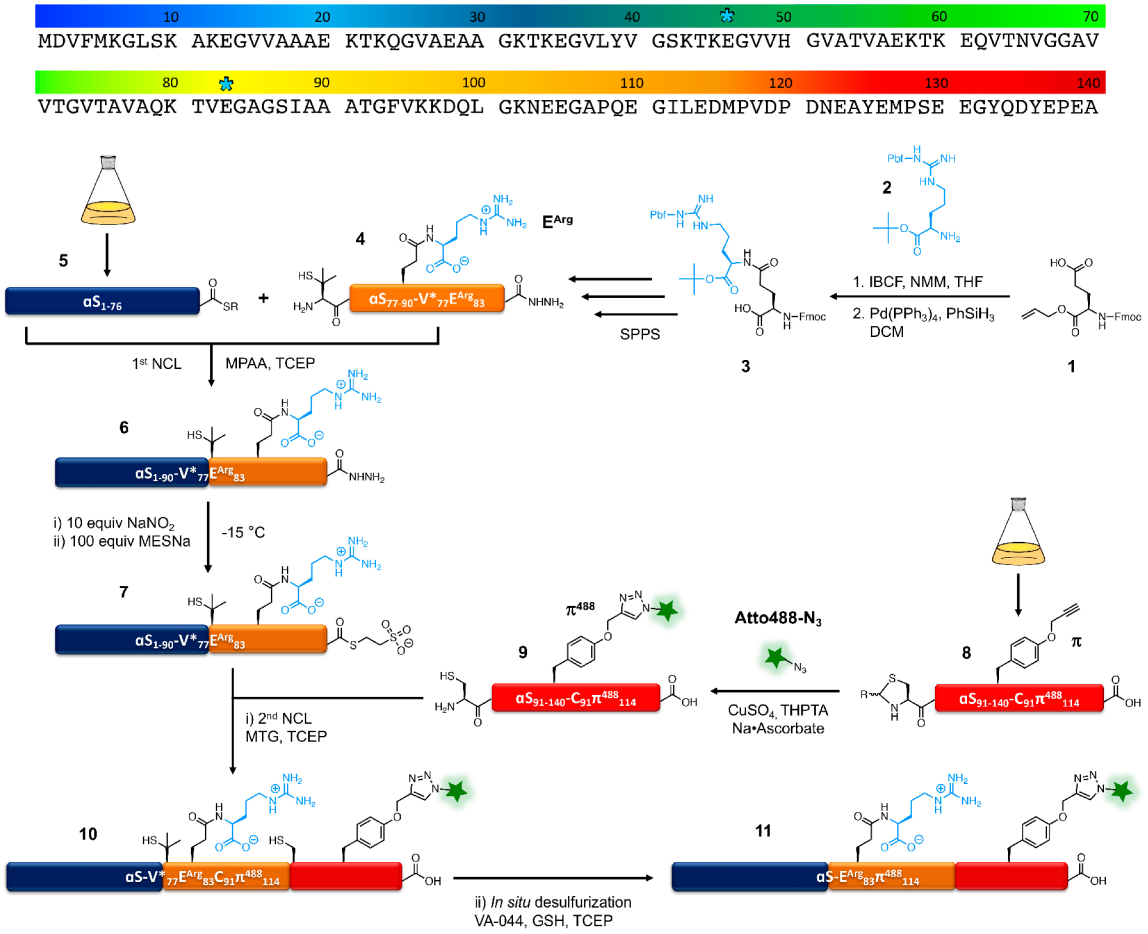

[a]Top: αS sequence with positions 46 and 83 indicated by ∗. Bottom: Synthesis of Fmoc-Glu(Arg(Pbf)-O^{t}Bu)-OH (**3**) and incorporation into αS fragments via SPPS, combined with unnatural amino acid mutagenesis, simultaneous "click" labeling and deprotection of the expressed protein fragment, and NCL for arginylated αS. The semisynthetic scheme for αS-E$^{Arg}_{83}\pi^{488}_{114}$ (**11**) is given as a representative example. Reaction conditions: NCL fragments dissolved to 2−3 mM final concentration, pH 7.0, incubation at 37 °C with agitation several hours to overnight, MESNa activation of ligation intermediate at room temperature with stirring for 15−20 min, desulfurization at 37 °C with agitation overnight. Details for reaction conditions and schemes for the synthesis of other constructs are given in Supporting Information.

none of the remaining Glu sites are expected to be modified), leading to increased aggregate formation and neurotoxicity.[6] Given that Glu46 and Glu83 are each found in one of the KTKEGV-type repeats of αS and that $E_{46}K$ mutations are associated with Parkinson's disease,[7,8] one study has also examined the effect of substituting these residues for a Lys or an Ala. The mutants, in particular, Ala46 and Ala83, were shown to increase αS fibrillization *in vitro*,[7] suggesting the importance of these amino acid positions in the assembly process, as well as the necessity of investigating the effect of an authentic arginylated glutamate at these positions.

Despite initial results suggesting the neuroprotective nature of arginylation, the PTM itself has not been studied in chemical detail. Here, we utilize site-specific incorporation strategies to directly examine the effect of arginylation at each position on αS lipid binding affinity and aggregation, respective *in vitro* models for αS function in health (modulating vesicle trafficking) and in the formation of pathological fibrils. Building on previous syntheses of αS bearing PTMs and/or probes (see comparison of methods in the Discussion section),[9−19] we develop several methods for the semisynthesis of αS bearing E^{Arg} at specific sites. To this end, we synthesize a protected E^{Arg} amino acid monomer for incorporation into full-length αS by solid phase peptide synthesis (SPPS) and native chemical ligation (NCL). We present the semisynthesis of various constructs of αS with E^{Arg} at site 46, site 83, or both, combined with an orthogonally installed fluorophore. We compare strategies and present an optimized synthetic strategy to produce various single E^{Arg} αS constructs, as well as a streamlined ligation strategy to access doubly arginylated αS. We demonstrate the synthesis of a novel ligation handle and its utility in a multistep ligation reaction. We determine by fluorescence correlation spectroscopy (FCS) and aggregation assays that arginylated αS binds to lipid vesicles with the same affinity as unmodified protein but reduces fibril formation, demonstrating the effects of this unusual PTM on αS function and behavior in disease.

RESULTS

Synthesis of E^{Arg} Monomer, SPPS, and Expression of Protein Fragments for NCL. To incorporate arginylated glutamate site-specifically, we developed several semisynthetic strategies corresponding to each construct (refer to Supporting Information Table S1 for a list of all peptide/protein constructs

https://dx.doi.org/10.1021/jacs.0c10054
J. Am. Chem. Soc. 2020, 142, 21786−21798

Scheme 2. NCL Strategy for the Synthesis of Doubly Arginylated αS[a]

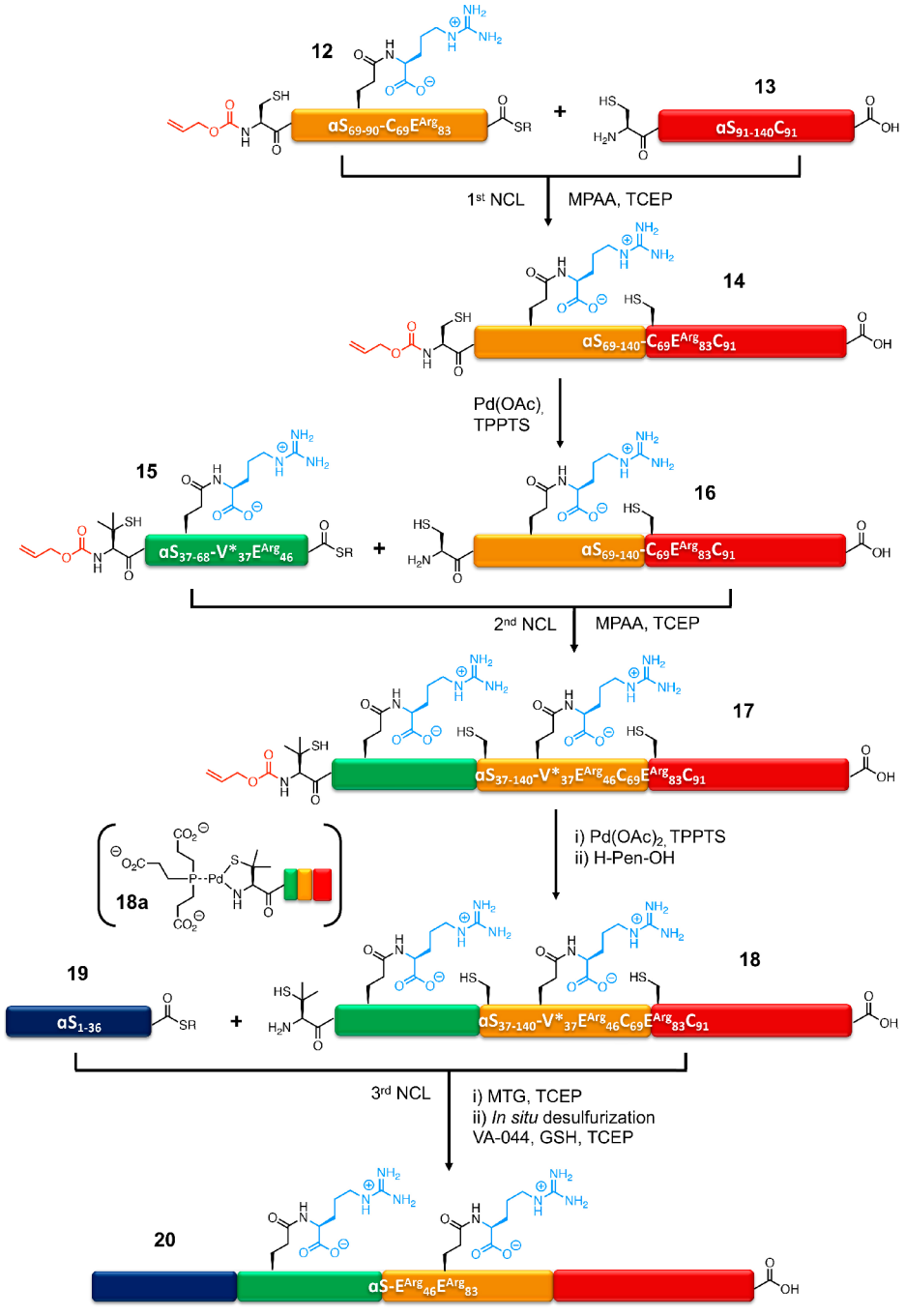

[a]The semisynthetic scheme for αS-E$^{Arg}_{46}$E$^{Arg}_{83}$ (**20**) is given as a representative example, illustrating the use of Alloc-protected Cys or Pen (red) and the final MTG-mediated ligation step. Reaction conditions: C-terminal fragment (**13** in this case) dissolved to 2 mM final concentration, 1.2–1.5 equiv of each subsequent fragment added relative to the preceding one, incubation at 37 °C with agitation for 3 h each, deprotection with 2 equiv of Pd to protein at 37 °C for 10 min, final NCL and desulfurization at 37 °C overnight. Details for reaction conditions and schemes for the synthesis of other constructs are given in Supporting Information.

and yields). First, we synthesized fluorenylmethyloxycarbonyl (Fmoc) and pentamethyldihydrobenzofuran-5-sulfonyl (Pbf) protected E^{Arg}, Fmoc-Glu(Arg(Pbf)-O^{t}Bu)-OH (**3**), for incorporation into peptides by SPPS. This PTM-bearing amino acid was synthesized from N-terminally Fmoc-protected, C-terminally allylated, but side-chain unprotected glutamate (Fmoc-Glu-OAll, **1**), and side-chain protected arginine (H-Arg(Pbf)-O^{t}Bu, **2**). Notably, after silica column purification including 0.125% acetic acid in the eluent, the combined fractions were azeotroped at least four times with toluene to completely remove acetic acid to avoid acetyl capping of the growing peptide during SPPS. Pure product **3** was obtained in 65% yield (Figure S1, Supporting Information).

The E^{Arg} precursor **3** was then used in SPPS to generate peptides for incorporation of the PTM into full-length αS (see Scheme 1 for the synthesis of αS-E$^{Arg}_{83}\pi^{488}_{114}$ (where π is propargyl tyrosine); see Schemes S1–S4 for the syntheses of

https://dx.doi.org/10.1021/jacs.0c10054
J. Am. Chem. Soc. 2020, 142, 21786–21798

other constructs). To synthesize αS with the E^{Arg} at residue 46, we divided the protein sequence into three segments. We synthesized αS_{77-90}-$V^*_{77}E^{Arg}_{83}$-$NHNH_2$ (**4**) bearing arginylated glutamate at position 83, a penicillamine (Pen, V*) ligation handle[20] that could be desulfurized after NCL to afford the native valine at position 77, and a C-terminal acyl hydrazide. Coupling of the Fmoc-Glu(Arg(Pbf)-O^{t}Bu)-OH amino acid **3** was carried out at 37 °C using 2 equiv of amino acid, 2 equiv of 7-azabenzotriazol-1-yloxy)tripyrrolidinophosphonium hexafluorophosphate (PyAOP), and 4 equiv of *N*,*N*-diisopropylethylamine (DIPEA) and proceeded to completion after single coupling, as confirmed by Kaiser test, but was doubly coupled for good measure. Coupling of trityl-protected penicillamine (Fmoc-Pen(Trt)-OH) was effective when carried out using HBTU as previously described,[16] but for consistency of coupling agent used in one peptide, we also employed alternative conditions, which consisted of stirring 4 equiv of amino acid at a concentration of 0.4 M with 4 equiv of PyAOP, 4 equiv of HOBt, and 8 equiv of DIPEA at 60 °C for 1 h. Pure peptide αS_{77-90}-$V^*_{77}E^{Arg}_{83}$-$NHNH_2$ **4** was obtained in 28% yield (Figure S3, Supporting Information). The N-terminal fragment αS_{1-76} was expressed as an intein fusion, which was cleaved with sodium 2-mercaptoethanesulfonate (MESNa) to convert the fragment to a thioester (αS_{1-76}-MES, **5**, 24.1 mg per L of culture) for ligation. For the C-terminal fragment of the protein, we expressed a fragment of the native protein to synthesize unlabeled, arginylated αS as well as a fluorescently labeled version to synthesize an arginylated αS for biophysical studies. For the unlabeled construct, fragment αS_{91-140}-C_{91} (**13**, Scheme 2 and Scheme S3, Supporting Information) was expressed as a deletion construct as previously described, and the thiazolidine formed from intracellular methionine aminopeptidase activity was deprotected using methoxyamine to expose the reactive cysteine for NCL (yield = 15.4 mg per L of *E. coli* culture). To generate a fluorescently labeled construct, we expressed the same fragment with an unnatural amino acid, propargyl tyrosine (π), at position 114 using amber codon suppression,[21] in order to attach the fluorophore Atto 488 via click chemistry,[22,23] affording the fragment αS_{91-140}-$C_{91}\pi^{488}_{114}$ (**9**, yield = 8.5 mg per L of culture). Similarly, to synthesize full-length αS with an arginylated glutamate at residue 46 (Schemes S1 and S2, Supporting Information), we expressed αS_{1-36} as a MES thioester (**19**, yield = 13.7 mg per L of culture), synthesized αS_{37-55}-$V^*_{37}E^{Arg}_{46}$-$NHNH_2$ (**S3**) via SPPS as an acyl hydrazide (19% yield), and recombinantly produced an unlabeled αS_{56-140}-C_{56} (**S7**, yield = 17.9 mg per L of culture) and a fluorescent αS_{56-140}-$C_{56}\pi^{488}_{114}$ (**S11**, yield = 2.6 mg per L of culture) for use in NCL.

Role of Copper in the Deprotection, Click Labeling, and Oxidation of Peptides. In generating the fluorescent C-terminal fragments of αS for the synthesis of both the E^{Arg}_{46} and the E^{Arg}_{83} constructs, we observed some interesting phenomena regarding the reactivity of copper toward the peptides. Each fragment, such as αS_{56-140}-$C_{56}\pi_{114}$ **S10** and αS_{91-140}-$C_{91}\pi_{114}$ **8**, was expressed as a thiazolidine-protected fragment and deprotected using methoxyamine. Since the thiazolidines are formed in cells after cleavage of the initiator methionine followed by reactions with various carbonyl compounds present in the cell, we observed that both the native and the π-bearing purified fragments were protected by a mixture of thiazolidines formed from formaldehyde, acetaldehyde, pyruvate, and other aldehydes. In all cases, the methoxyamine reaction afforded a clean deprotection to reveal the reactive cysteine (Figure S10, Supporting Information). When we then attempted to label the purified π-bearing peptide using Atto 488-azide and a catalytic mixture consisting of 2 equiv of copper sulfate, 10 equiv of tris(3-hydroxypropyltriazolylmethyl)amine (THPTA), and 20 equiv sodium ascorbate, we observed a mass of +16 Da higher than the expected mass using matrix-assisted laser desorption ionization (MALDI) mass spectrometry (MS) (Figure S10, Supporting Information). It appears that the additional mass corresponded to the oxidation of the N-terminal cysteine, as the peptide was unreactive in NCL. This result was surprising, as previously reported interactions between copper and N-terminal cysteine[24] show that in the presence of sodium ascorbate, N-terminal cysteine of a peptide does not undergo oxidation even in the absence of a protective disulfide-forming internal cysteine. Since copper has been reported to be able to deprotect thiazolidines[24] and selenazolidines,[25] we employed an alternative strategy whereby purified, thiazolidine-protected αS_{91-140}-$C_{91}\pi_{114}$ was simultaneously deprotected and click labeled using the copper catalytic mixture.[26] The thiazolidine-protected peptide was dissolved in argon-sparged buffer, fluorophore-azide and catalytic mixture were added, and the reaction was degassed again and incubated in the dark at 37 °C for 15 min. The copper catalytic mixture was able to deprotect all thiazolidines except for pyruvate-derived thiazolidines. The copper was also able to simultaneously catalyze the click labeling of an azide derivative of the Atto 488 dye (Atto488-N_3) onto the protein fragment (Figure S11, Supporting Information). A small amount of oxidation of deprotected cysteine was still observed by MALDI-MS even though complete suppression of oxidation was seen in previous reports using CuCl to deprotect thiazolidine under argon atomosphere[25] or using $CuSO_4$ and ascorbate under ambient atmosphere.[24] Nevertheless, when we conducted the simultaneous click and deprotection reaction in an anaerobic chamber, the side product was not detectable by analytical high-performance liquid chromatography (HPLC), indicating that it was not produced in significant amounts (Figure S13, Supporting Information). Pure preparative HPLC fractions of labeled, deprotected αS_{91-140}-$C_{91}\pi^{488}_{114}$ (**9**) were kept for later use in NCL, whereas fractions of labeled, pyruvate-derived thiazolidine-protected αS_{91-140}-$C_{91}\pi^{488}_{114}$ were pooled and subjected to another round of deprotection mediated by methoxyamine (Figure S12, Supporting Information). This reaction afforded cleanly deprotected αS_{91-140}-$C_{91}\pi^{488}_{114}$ (**9**, 59% yield over all steps). The same was done for αS_{56-140}-$C_{56}\pi^{488}_{114}$ (**S11**, 41% yield over all steps).

Native Chemical Ligation To Produce αS E^{Arg}_{46} and E^{Arg}_{83}. To generate full-length αS bearing E^{Arg} at residue 83, we performed NCL between the αS_{1-76}-MES thioester (**5**) and αS_{77-90}-$V^*_{77}E^{Arg}_{83}$ hydrazide peptide (**4**). Although the Ala_{76} thioester was unhindered, the steric bulk of V^*_{77} required the reaction to be incubated overnight. After HPLC purification, the intermediate was obtained in 61% yield (Figure S20, Supporting Information). This ligated fragment, αS_{1-90}-$V^*_{77}E^{Arg}_{83}$, was then ligated to αS_{91-140}-C_{91} by *in situ* conversion of the αS_{1-90}-$V^*_{77}E^{Arg}_{83}$ acyl hydrazide (**6**) to a thioester using 4-mercaptophenylacetic acid (MPAA). Following HPLC purification (32% yield), the penicillamine and cysteine ligation handles were desulfurized to the respective valine and alanine, and the products were purified (15% yield). Full-length αS-E^{Arg}_{83} (**S16**) product was obtained in 2.4%

https://dx.doi.org/10.1021/jacs.0c10054
J. Am. Chem. Soc. 2020, 142, 21786−21798

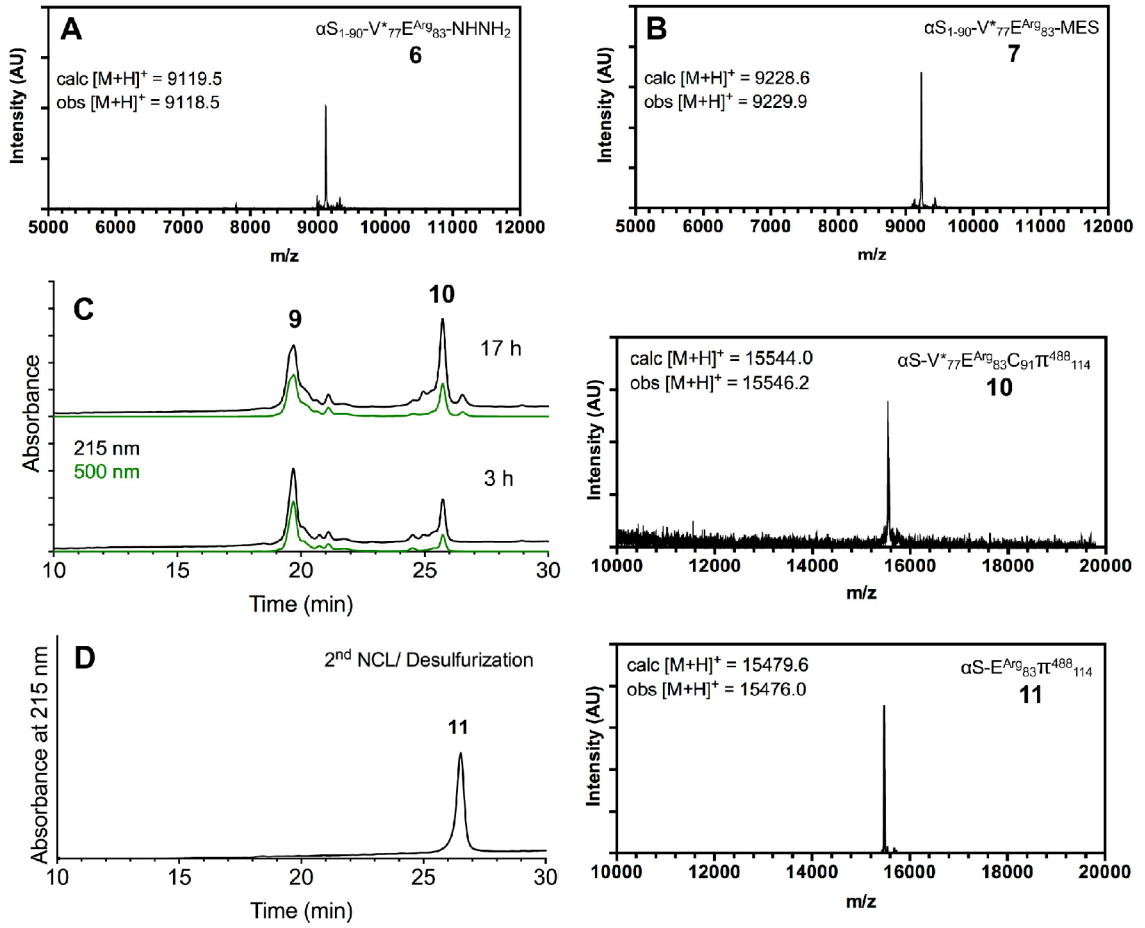

Figure 1. Synthesis of αS-E$^{Arg}_{83}\pi^{488}_{114}$: (A) MALDI-MS of product αS_{1-90}-V*$_{77}$E$^{Arg}_{83}$-NHNH$_2$ (**6**) resulting from NCL between αS_{1-76}-MES (**5**) and αS_{77-90}-V*$_{77}$E$^{Arg}_{83}$-NHNH$_2$ (**4**); (B) MALDI-MS of conversion of intermediate **6** to αS_{1-90}-V*$_{77}$E$^{Arg}_{83}$-MES (**7**); (C) analytical HPLC (gradient, 10−50% B over 30 min) of MTG-mediated NCL between αS_{1-90}-V*$_{77}$E$^{Arg}_{83}$-MES (**7**) and αS_{91-140}-C$_{91}\pi^{488}_{114}$ (**9**) to give αS-V*$_{77}$E$^{Arg}_{83}$C$_{91}\pi^{488}_{114}$ (**10**); (D) analytical HPLC of *in situ* desulfurized product αS-E$^{Arg}_{83}\pi^{488}_{114}$ (**11**).

overall yield (Figure S21, Supporting Information). The same strategy was executed to produce αS-E$^{Arg}_{46}$ (**S9**). Ligation between αS_{1-36}-MES (**19**) and αS_{37-55}-V*$_{37}$E$^{Arg}_{46}$ hydrazide (**S3**) produced the intermediate αS_{1-55}-V*$_{37}$E$^{Arg}_{46}$ hydrazide (**S4**) in 79% yield (Figure S14, Supporting Information). Over all steps, full length unlabeled αS E$^{Arg}_{46}$ (**S9**) was obtained in 4.1% yield (Figure S15, Supporting Information).

Comparison of Aryl vs Alkyl Thiol Additives in Hydrazide Conversion NCL. To improve upon these yields, we tested an alternative strategy that allowed for the second ligation and desulfurization to be done *in situ*. A previous report demonstrated that an alternative thiol additive, methyl thioglycolate (MTG), can be used to generate the C-terminal thioesters of protein fragments and allows for desulfurization without purification of the ligation product.[27] We therefore attempted to use MTG as the thiol additive in place of MPAA in the second ligation so as to bypass a purification step between this ligation and the desulfurization, which we thought may improve the yield. We dissolved the intermediate fragment αS_{1-55}-V*$_{37}$E$^{Arg}_{46}$-NHNH$_2$ (**S4**) in pH 3 buffer, activated the acyl hydrazide using 10 equiv of NaNO$_2$, followed by addition of 100 equiv of MTG (as a neutral buffered solution) in place of MPAA. After the partner peptide (αS_{56-140}-C$_{56}$ **S7**) was added to the reaction, we examined the sample by MALDI-MS and observed product formation after 3 h. However, we also observed various additional masses on the remaining αS_{56-140}-C$_{56}$ fragment (Figure S16, Supporting Information). Importantly, these additional masses were not incorporated into the product, indicating the possible formation of oxidization adducts on the N-terminal cysteine ligation handle. In the previously reported case study, the researchers preconverted the peptides of interest into MTG thioesters and purified them before use in ligation with the C-terminal fragment[27] so that no free cysteine was present in the same pot as NaNO$_2$.

We therefore instead opted to convert the intermediate product, αS_{1-55}-V*$_{37}$E$^{Arg}_{46}$ acyl hydrazide (**S4**) into a MES thioester (**S5**), which is known to be a stable thioester, and purify it before use in the second ligation. Although this strategy introduced another purification step before the second ligation, its compatibility with *in situ* desulfurization allowed us to forgo a purification step after the ligation and importantly to recover more product by reducing the number of times the full-length αS is purified or lyophilized, as it is more aggregation-prone than the N-terminal fragments. The hydrazide to MES thioester conversion always proceeded to completion and was isolated in 85% yield (Figure S17, Supporting Information). *In situ* conversion of the MES thioester to MTG thioester in the NCL reaction was rapid, and despite the known slower reactivity of MTG compared to MPAA, compounded by the steric bulk of the V$_{55}$ thioester under attack, our MTG-mediated NCL was complete after

https://dx.doi.org/10.1021/jacs.0c10054
J. Am. Chem. Soc. 2020, 142, 21786−21798

overnight incubation. Overall, this route allowed us to isolate desulfurized, unlabeled αS-E^{Arg}_{46} (**S9**) in 14.4% yield (Figure S18, Supporting Information) and fluorescent αS-$E^{Arg}_{46}\pi^{488}_{114}$ (**S13**) in 37.7% yield (Figure S19, Supporting Information), representing an improvement over the MPAA-mediated ligation strategy. Encouraged by this, we used the same strategy to produce αS arginylated at residue 83. After ligation between αS_{1-76} MES thioester (**5**) and αS_{77-90}-$V^*_{77}E^{Arg}_{83}$ (**4**), the conversion of the αS_{1-90}-$V^*_{77}E^{Arg}_{83}$ hydrazide intermediate (**6**) to the MES thioester (**7**) proceeded to completion and was isolated in 87.5% yield (Figure S22, Supporting Information). The MTG-mediated approach resulted in unlabeled αS-E^{Arg}_{83} (**S16**) in 32.5% yield (Figure S23, Supporting Information) and fluorescent αS-$E^{Arg}_{83}\pi^{488}_{114}$ (**11**) in 15.4% yield over all steps (Figure 1 and Figure S24, Supporting Information), demonstrating once again the superiority of the method amenable to desulfurization without intermediate purification.

Generation of Peptides for Synthesis of Doubly Arginylated αS. In order to study the combined effects of arginylation at both positions 46 and 83, we synthesized full-length constructs simultaneously bearing E^{Arg} at both sites. To this end, we developed a streamlined C-to-N terminal synthetic scheme inspired by a previously published one-pot ligation strategy for histone total synthesis.[28] We divided full-length αS into four segments for ligation: αS_{1-36}, αS_{37-68}, αS_{69-90}, and αS_{91-140}. Capitalizing on the existence of αS_{1-36} MES thioester (**19**) and αS_{91-140}-C_{91} (**13**) or αS_{91-140}-$C_{91}\pi^{488}_{114}$ (**9**) constructs from our syntheses of singly arginylated αS, we produced these fragments for the synthesis of doubly arginylated αS as well. As for fragments bearing our PTM of interest, we targeted the synthesis of αS_{37-68}-$V^*_{37}E^{Arg}_{46}$ and αS_{69-90}-$C_{69}E^{Arg}_{83}$ as N-terminally allyloxycarbonyl- (Alloc-) protected peptides so that they could be added sequentially in one-pot reactions. We chose Val37 as the ligation site so as to make all of the protein segments an appropriate length. Another ligation site that is nearby would be Ala30, but this would require the use of αS_{30-68} for the fragment containing arginylated glutamate at position 46 which is likely to be lower yielding. For similar reasons, we chose to divide αS into four fragments since this was the minimal number of fragments that would allow for incorporation of E^{Arg} at positions 46 and 83 while keeping each peptide fragment at a reasonable length for good yield.

To synthesize the appropriate fragment peptides, we carried out the synthesis of Alloc-Cys(Trt)-OH (**S1**, Supporting Information Scheme S4) as previously described.[28] For the synthesis of Alloc-protected penicillamine, the starting material H-Pen(Trt)-OH was reacted with 1.5 equiv of allyl chloroformate in dioxane and 2% Na_2CO_3 in H_2O, as in the synthesis of Alloc-Cys(Trt)-OH. Formation of Alloc-Pen(Trt)-OH (**S2**, Supporting Information Scheme S4) proceeded to completion in 1 h. In contrast to the synthesis of its cysteine counterpart, the crude reaction mixture of Alloc-Pen(Trt)-OH was not acidified with HCl, as the end point pH was measured to be at pH 3−4. After workup, Alloc-Pen(Trt)-OH was obtained in quantitative yield, and the product could be used for SPPS without further purification (Figure S25, Supporting Information).

Using our Alloc-amino acids and Fmoc-Glu(Arg(Pbf)-O^{t}Bu)-OH**3**, we synthesized the Alloc-αS_{37-68}-$V^*_{37}E^{Arg}_{46}$ (**15**) and Alloc-αS_{69-90}-$C_{69}E^{Arg}_{83}$ (**12**) peptides as C-terminal acyl hydrazides. Owing to the steric bulk of its β-branching and side-chain protection, Alloc-Pen(Trt)-OH coupling was incomplete under standard conditions (double coupling at room temperature for 30 min). We found that optimal coupling resulted from double coupling 4 equiv of Alloc-Pen(Trt)-OH**S2** using 4 equiv of PyAOP, 4 equiv of ethyl cyano(hydroxyimino)acetate (Oxyma Pure), 4 equiv of hydroxybenzotriazole (HOBt), and 8 equiv of DIPEA at 37 °C for 1 h. Using these conditions, SPPS of Alloc-αS_{37-68}-$V^*_{37}E^{Arg}_{46}$ **15** was achieved. After the acyl hydrazide peptide was cleaved from resin and precipitated with ether, the dried precipitate was redissolved in 0.2 M sodium phosphate buffer at pH 3 and converted to a stable thioester using 10 equiv of $NaNO_2$ and 100 equiv of MESNa. The conversion proceeded to completion, and the peptide thioester was purified by HPLC and isolated in 14.8% yield overall (Figure S26, Supporting Information). Similarly, Alloc-αS_{69-90}-$C_{69}E^{Arg}_{83}$ **12** was synthesized, with coupling of Alloc-Cys(Trt)-OH **S1** done under standard conditions. However, upon addition of 0.2 M sodium phosphate buffer to the dried ether precipitate, the peptide formed a gel that was irreversible, despite our attempts through addition of denaturant, purification, or lyophilization and resolvation. We reasoned that this was because fragment 69−90 consists of the non-amyloid-β component (NAC) of αS, a region abundant with hydrophobic residues making it prone to aggregation.[29] Therefore, we adopted an alternative strategy whereby the dried ether precipitate of Alloc-αS_{69-90}-$C_{69}E^{Arg}_{83}$ acyl hydrazide **12** was redissolved in 6 M guanidinium and 0.2 M phosphate at pH 3 for the conversion to MESNa thioester. The reaction proceeded to completion in 15−20 min. The crude mixture was diluted to reduce the guanidinium concentration to <1.5 M and immediately purified by HPLC without filtration. Pure peptide was obtained in 19.6% yield over all steps (Figure S27, Supporting Information).

Semisynthesis of Doubly Arginylated αS $E^{Arg}_{46}E^{Arg}_{83}$. We used the Alloc-protected arginylated peptides along with the already available αS fragments to effectuate the semisynthesis of unlabeled and fluorescent doubly arginylated αS-$E^{Arg}_{46}E^{Arg}_{83}$ (Scheme 2 and Supporting Information, Scheme S4). Toward these doubly arginylated αS constructs, we carried out a streamlined sequence of C-to-N terminal NCL reactions by first ligating αS_{91-140}-C_{91} **13** (or αS_{91-140}-$C_{91}\pi^{488}_{114}$ **9**) with Alloc-αS_{69-90}-$C_{69}E^{Arg}_{83}$ MES thioester **12**. Upon completion of the ligation in 3 h, deprotection of Alloc-αS_{69-140}-$C_{69}E^{Arg}_{83}C_{91}$ **14** was carried out in the same pot using palladium acetate ($Pd(OAc)_2$) and 3,3′,3″-phosphanetriyltris-(benzenesulfonic acid) trisodium salt (TPPTS) ligand to give αS_{69-140}-$C_{69}E^{Arg}_{83}C_{91}$ **16** in 10 min. The next fragment, Alloc-αS_{37-68}-$V^*_{37}E^{Arg}_{46}$ MES thioester **15**, was added as a dry powder. Formation of the ligated product Alloc-αS_{37-140}-$V^*_{37}E^{Arg}_{46}C_{69}E^{Arg}_{83}C_{91}$ **17** was complete in 3 h, and Pd-catalyzed Alloc deprotection was performed again. Here, rather than completing the ligation sequence with the addition of αS_{1-36} MES thioester **19**, we developed an alternative strategy in which deprotected H_2N-αS_{37-140}-$V^*_{37}E^{Arg}_{46}C_{69}E^{Arg}_{83}C_{91}$ **18** was purified by HPLC and ligated to αS_{1-36} MES **19** in a separate pot. We opted for this strategy for two reasons. First, while the one-pot ligation required the use of MPAA to inactivate Pd before addition of the next fragment, the separate pot ligation with αS_{1-36} MES **19** allowed us to use MTG as a thiol additive, which permitted subsequent desulfurization without intermediate purification. This approach would result in the same total number of reaction vessels and purification steps, while affording some advantages: we could add more

https://dx.doi.org/10.1021/jacs.0c10054
J. Am. Chem. Soc. 2020, 142, 21786−21798

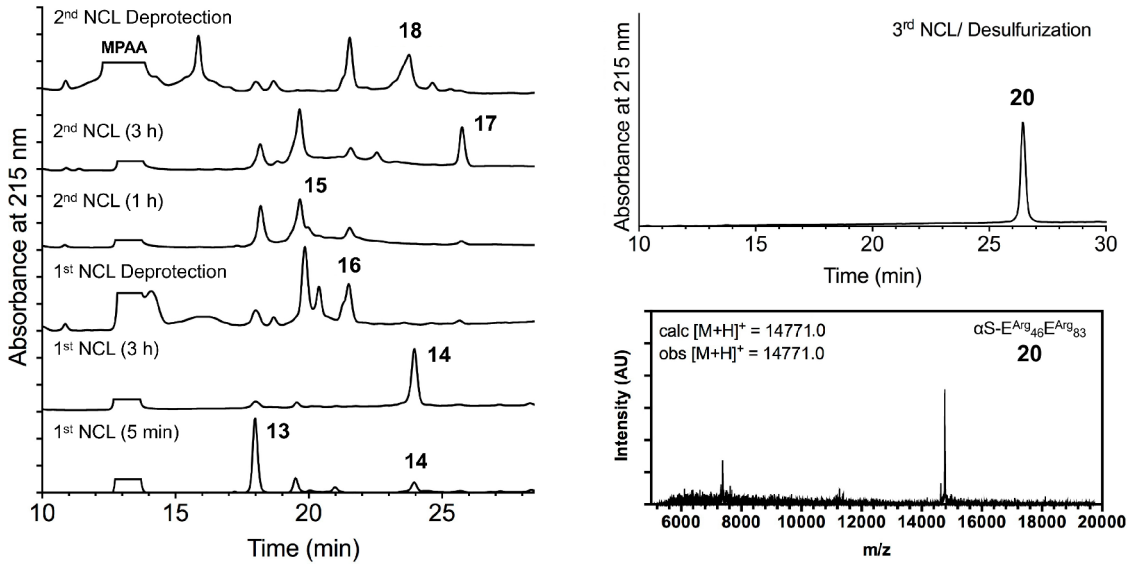

Figure 2. NCL for the synthesis of αS-$E^{Arg}_{46}E^{Arg}_{83}$ (**20**). Left: Analytical HPLC (gradient, 10−50% B over 30 min) of first NCL, between Alloc-αS_{69-90}-$C_{69}E^{Arg}_{83}$ (**12**) (elutes early and has minimal absorbance) and αS_{91-140}-C_{91} (**13**) to generate Alloc-αS_{69-140}-$C_{69}E^{Arg}_{83}C_{91}$ (**14**), first NCL Alloc deprotection to generate αS_{69-140}-$C_{69}E^{Arg}_{83}C_{91}$ (**16**), second NCL between **16** and Alloc-αS_{37-68}-$V^*_{37}E^{Arg}_{46}$ (**15**) to generate Alloc-αS_{37-140}-$V^*_{37}E^{Arg}_{46}C_{69}E^{Arg}_{83}C_{91}$ (**17**), and second Alloc deprotection to generate αS_{37-140}-$V^*_{37}E^{Arg}_{46}C_{69}E^{Arg}_{83}C_{91}$ (**18**). Top right: Analytical HPLC of product αS-$E^{Arg}_{46}E^{Arg}_{83}$ (**20**) after third NCL between αS_{1-36}-MTG thioester (**19**) and **18**, followed by desulfurization and preparative HPLC purification. Bottom right: MALDI-MS analysis of purified **20**.

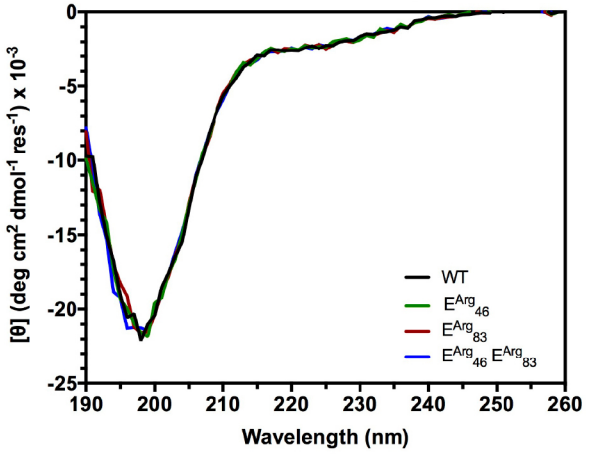

αS Variant	Diffusion time (ms)	Norm. CPM
WT	0.52 ± 0.01	0.51 ± 0.04
E^{Arg}_{46}	0.52 ± 0.02	0.50 ± 0.02
E^{Arg}_{83}	0.50 ± 0.01	0.48 ± 0.03
E^{Arg}_{46} E^{Arg}_{83}	0.53 ± 0.02	0.46 ± 0.04

Figure 3. Structure and monomeric state of arginylated αS vs control. Left: CD spectra of αS E^{Arg}_{46}, E^{Arg}_{83}, or $E^{Arg}_{46}E^{Arg}_{83}$ in comparison to WT αS, with characteristic negative Cotton effect at 200 nm indicative of random coil. Right: Diffusion time and normalized counts per molecule (CPM) of fluorescently labeled αS-π^{488}_{114} WT control, $E^{Arg}_{46}\pi^{488}_{114}$, $E^{Arg}_{83}\pi^{488}_{114}$, or $E^{Arg}_{46}E^{Arg}_{83}\pi^{488}_{114}$, determined by FCS. For protein in buffer without lipids, 10 autocorrelation curves were averaged in each measurement, and measurement sets were performed in independent triplicates. Primary FCS data are shown in Supporting Information, Figure S33.

than 1.2 equiv of peptide for each sequential ligation to totally consume the C-terminal fragment, which was the limiting reagent (especially αS_{91-140}-$C_{91}\pi^{488}_{114}$ **9**, bearing a fluorophore), and we could also reduce the number of times the full-length αS is lyophilized, maximizing recovery of the final product. The second reason for which we adopted the multipot ligation-and-desulfurization strategy was that we observed an unusual interaction between Pd and penicillamine. In the Alloc deprotection procedure, upon completion of deprotection by Pd-TPPTS, TCEP is added to inactivate the catalyst. In the cases of both Alloc-cysteine and Alloc-penicillamine peptides, deprotection was complete in 10 min; the reaction mixture was incubated with TCEP for an additional 10 min, and the sample was ready for the next ligation. However, in the case of the Alloc-penicillamine αS_{37-140} fragments (e.g., conversion of **17** to **18**), we observed an additional mass of +357 on the peptide which rendered it unreactive to αS_{1-36}, suggesting that a TCEP·Pd adduct had formed on the ligation handle (Scheme 2, **18a**; see also Figure S32, Supporting Information). The additional mass was not removed by addition of 1,4-dithiothreitol (DTT), ethanedithiol (EDT), or other bidentate ligands. However, upon addition of 1 equiv of free penicillamine amino acid (H-Pen-OH), the additional mass was eliminated, resulting in reactive αS_{37-140} fragments (Figure S32, Supporting Information). We hypothesize that upon Alloc deprotection and inactivation of Pd by TCEP, the N-terminal penicillamine coordinated Pd-TCEP in a rigid five-membered structure (**18a**) because of the Thorpe−Ingold effect[30,31]

https://dx.doi.org/10.1021/jacs.0c10054
J. Am. Chem. Soc. 2020, 142, 21786−21798

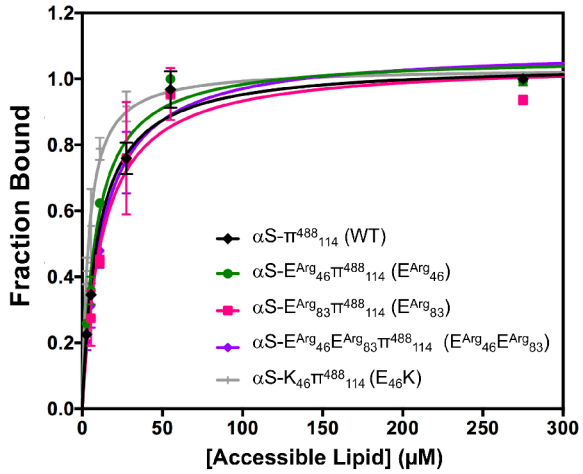

αS Variant	$K_{d,app}$ (μM)
WT	9.8 ± 1.0
E^{Arg}_{46}	8.9 ± 1.0
E^{Arg}_{83}	12.8 ± 2.7
$E^{Arg}_{46}E^{Arg}_{83}$	11.9 ± 2.2
$E_{46}K$	4.4 ± 0.5

Figure 4. Vesicle binding affinity of αS. All arginylated αS variants display comparable apparent dissociation constants ($K_{d,app}$), suggesting that arginylation does not alter the native role of αS. The disease mutant αS-K_{46} displays enhanced binding, consistent with literature. Primary FCS data and individual binding curves are shown in Supporting Information, Figures S35 and S36.

afforded by its two β-carbon methyl groups which are absent in the N-terminal cysteine and the common bidentate ligands. Thus, the αS_{37-140} intermediate products were purified in 35.2% yield for unlabeled αS (**18**, Figure S28, Supporting Information) and 41.7% yield for fluorescent αS (**S20**, Figure S29, Supporting Information). In a separate pot, these fragments were ligated to αS_{1-36} **19** using MTG and desulfurized. The semisyntheses resulted in unlabeled αS-$E^{Arg}_{46}E^{Arg}_{83}$ **20** in 6.1% yield (Figure 2 and Figure S29, Supporting Information) and fluorescent αS-$E^{Arg}_{46}E^{Arg}_{83}\pi^{488}_{114}$ **S21** in 7.2% yield over all steps (Figure S31, Supporting Information).

Arginylated αS Is Monomeric and Disordered, Similar to Wild Type (WT) αS. After synthesis of our various αS constructs, we investigated whether arginylation altered the secondary structure of αS by circular dichroism (CD) spectroscopy. Each singly and doubly arginylated αS was compared to WT in phosphate buffer, pH 7.4. The spectrum of each variant displays the same negative Cotton effect at 200 nm, characteristic of a random coil, indicating that no significant secondary structure was induced by the arginylation modifications (Figure 3, left). We also verified that the arginylated αS proteins are monomeric by FCS, like wild type (WT) αS. Fluorescence emission was collected from singly arginylated αS-$E^{Arg}_{46}\pi^{488}_{114}$ (**S13**) or αS-$E^{Arg}_{83}\pi^{488}_{114}$ (**11**) or from doubly arginylated αS-$E^{Arg}_{46}E^{Arg}_{83}\pi^{488}_{114}$ (**S21**) diffusing through the focal volume, and the resulting autocorrelated signals were fit to an autocorrelation function consisting of a single diffusing species. Diffusion time is a physically relevant output parameter in FCS that allows for relative comparisons of particle size when measured on the same system. All arginylated αS constructs were characterized by the same diffusion time (~0.5 ms) as that of the WT control αS-π^{488}_{114}, demonstrating their monomeric nature (Figure 3, right). Furthermore, we calculated the counts per molecule (CPM) of each αS, which represents the amount of fluorescence detected per particle; oligomeric proteins are expected to have higher CPM. The CPM was obtained by dividing the average intensity of the measured signal by the number of molecules in the focal volume and normalized to the CPM of a freely diffusing fluorescent standard, Alexa Fluor 488. These normalized CPMs were the same for all arginylated αS and control, showing that each particle traversing the focal volume carries one fluorophore and therefore that each arginylated αS is monomeric.

Lipid Binding Measurements Suggest That Arginylation Does Not Perturb αS Native Function. Next, we investigated the effect of arginylation on the interactions of αS with lipid vesicles, measurements that often serve as a surrogate for αS function. Since αS has a high affinity for negatively charged lipid vesicles, we synthesized vesicles composed of 50:50 1-palmitoyl-2-oleoyl-*sn*-glycero-3-phospho-L-serine (POPS) and 1-palmitoyl-2-oleoyl-*sn*-glycero-3-phosphocholine (POPC). Vesicle size distribution was centered around ~80 nm in diameter, and samples were monodisperse, as verified by dynamic light scattering (Figure S34, Supporting Information). We then assayed the lipid binding affinity of our arginylated αS constructs by FCS, using αS-π^{488}_{114} as a WT control. To various concentrations of lipid vesicles were added 20 nM singly arginylated αS-$E^{Arg}_{46}\pi^{488}_{114}$ (**S13**) or αS-$E^{Arg}_{83}\pi^{488}_{114}$ (**11**) or doubly arginylated αS-$E^{Arg}_{46}E^{Arg}_{83}\pi^{488}_{114}$ (**S21**). The respective characteristic diffusion times of protein and vesicle were measured beforehand and fixed to these known quantities in the fitting of the two-component data. The fraction of protein bound to vesicle was obtained from these fits.[32] We found that, in comparison to control, all of the arginylated αS variants have essentially the same affinity for the lipid vesicles, suggesting that this PTM does not alter the native role of αS (Figure 4). The apparent dissociation constants ($K_{d,app}$) obtained from the binding curves were 9.8 ± 1.0 μM accessible lipid for WT (αS-π^{488}_{114}), 8.9 ± 1.0 μM for E^{Arg}_{46} (αS-$E^{Arg}_{46}\pi^{488}_{114}$, **S13**), 12.8 ± 2.7 μM for E^{Arg}_{83} (αS-$E^{Arg}_{83}\pi^{488}_{114}$, **11**), and 11.9 ± 2.2 μM for the doubly arginylated $E^{Arg}_{46}E^{Arg}_{83}$ protein (αS-$E^{Arg}_{46}E^{Arg}_{83}\pi^{488}_{114}$, **S21**). For comparison, it is known that the disease mutation $E_{46}K$ enhances the binding of αS to lipid vesicles.[32−34] Consistent with previous observations, we found that αS-$K_{46}\pi^{488}_{114}$ displayed enhanced binding to our synthetic vesicles ($K_{d,app}$ = 4.4 ± 0.5 μM) in comparison to control.

Arginylation Decelerates Aggregation and Reduces Incorporation of αS into Fibrils. In addition to the effects on the native role of αS, we wished to examine the purported protective effects of arginylation against disease. To this end, we assayed the kinetics and thermodynamics of the aggregation

https://dx.doi.org/10.1021/jacs.0c10054
J. Am. Chem. Soc. 2020, 142, 21786−21798

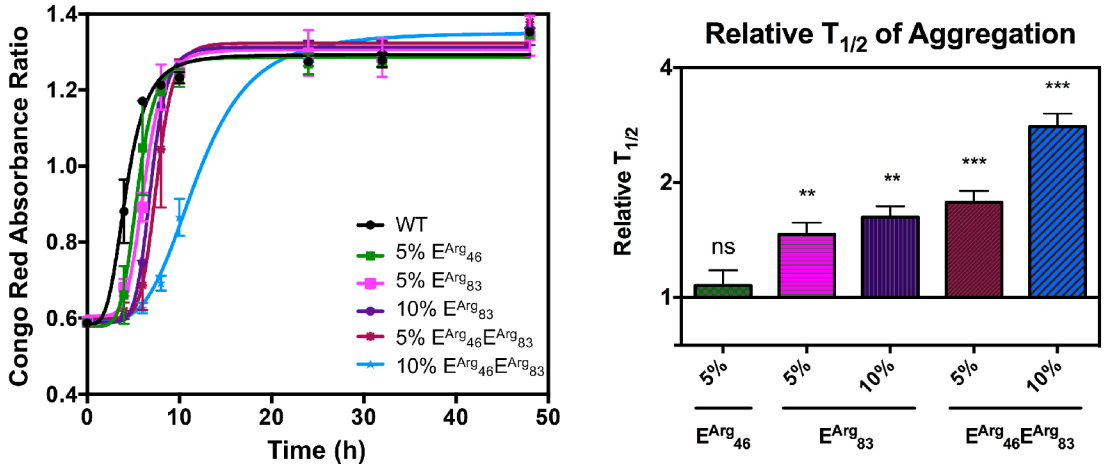

Figure 5. Aggregation kinetics for singly and doubly arginylated αS. αS monomers consisting of WT mixed with different percentages of αS-E^{Arg} were aggregated by agitation at 37 °C. The extent of aggregation was monitored by absorption of Congo Red. Left: Arginylation at glutamate 83 slows down aggregation of αS in a dose-dependent manner, and doubly arginylated αS E$^{Arg}_{46}$E$^{Arg}_{83}$ slows down aggregation more than E$^{Arg}_{83}$ alone. Individual aggregation curves are shown in Supporting Information, Figure S37. Right: $T_{1/2}$ values determined relative to WT value. Results are shown as the mean with standard error (n = 3): *p < 0.05; **p < 0.01; ***p < 0.001; ns, not significant.

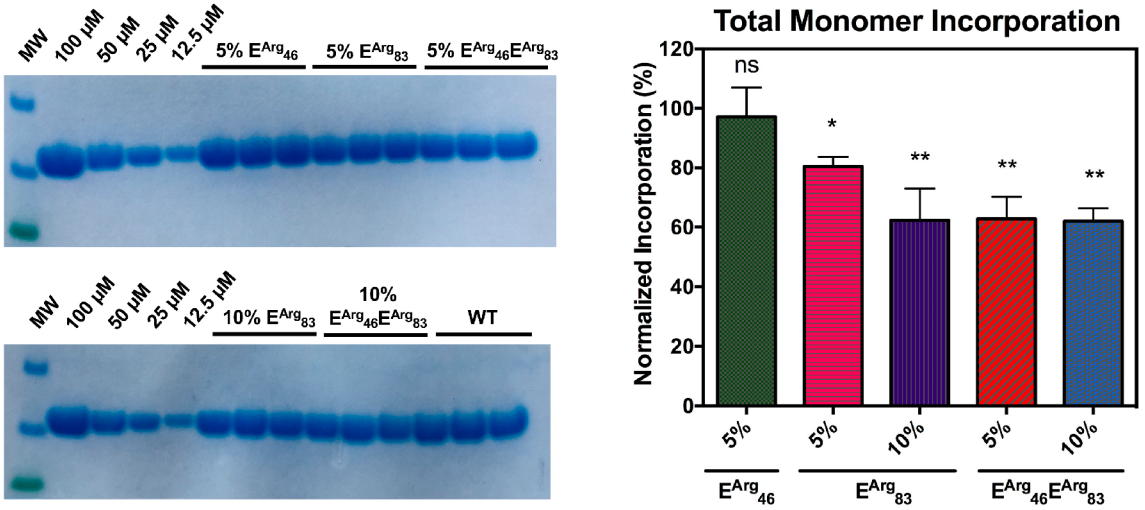

Figure 6. Percentage monomer incorporation for singly and doubly arginylated αS. αS monomers consisting of WT mixed with different percentages of αS-E^{Arg} were aggregated by agitation at 37 °C. End point samples were centrifuged, and pelleted fibrils were quantified by gel band density to determine percentage monomer incorporation. Left: Representative gel data showing standards used for quantification. Right: αS E$^{Arg}_{83}$ decreases the percentage incorporation of monomer into fibrils. Results are shown as the mean with standard error ($n \geq 3$): *p < 0.05; **p < 0.01; ns, not significant.

of arginylated αS. To test the impact of arginylation on aggregation kinetics, we prepared samples of 100 μM protein monomer in buffer (20 mM Tris, 100 mM NaCl, pH 7.4) consisting of wild type αS (unlabeled) or WT mixed with different percentages of αS-E$^{Arg}_{46}$ (**S9**) or αS-E$^{Arg}_{83}$ (**S16**) or the doubly arginylated αS-E$^{Arg}_{46}$E$^{Arg}_{83}$ (**20**). Samples were aggregated *in vitro* by agitating at 37 °C at 13 000 rpm, and the extent of aggregation was monitored by absorption of Congo Red in samples at various time points. We found that arginylation at glutamate 83 slows down aggregation and decreases the percentage incorporation of monomer into fibrils in a dose-dependent manner, with 10% E$^{Arg}_{83}$ exhibiting a greater effect than 5% E$^{Arg}_{83}$. On the other hand, E$^{Arg}_{46}$ showed no difference in aggregation kinetics in comparison to WT. Interestingly, the doubly arginylated protein E$^{Arg}_{46}$E$^{Arg}_{83}$ slowed down aggregation more than E$^{Arg}_{83}$ alone, suggesting that the compound effect of double arginylation was more significant than a simple additive effect of the individual arginylations (Figure 5).

To determine the effect of arginylation on the thermodynamic aspects of aggregation, we examined the percentage of starting monomer incorporated into the final fibrils in each sample. At the 48 h time point, samples were each centrifuged to pellet the fibrils. Supernatant containing any unincorporated monomer was discarded, and the fibrils were resuspended and quantified by the intensity of bands on a polyacrylamide (SDS−PAGE) gel. We found that when the starting material contained higher levels of arginylated αS, total incorporation of monomer into fibril was decreased (Figure 6). This effect was seen most strongly for the 83 position. While E$^{Arg}_{46}$ again showed no difference in monomer incorporation, the doubly arginylated E$^{Arg}_{46}$E$^{Arg}_{83}$ protein decreased incorporation to a similar extent to E$^{Arg}_{83}$, suggesting that most of the protective effect may be attributed to the 83 site.

https://dx.doi.org/10.1021/jacs.0c10054
J. Am. Chem. Soc. 2020, 142, 21786−21798

DISCUSSION

In this study, we report the first synthesis of αS bearing arginylation, an unusual PTM, and the generation of singly arginylated and doubly arginylated αS as well as variants bearing a fluorophore for biophysical studies. To accomplish this, we developed the synthesis of the novel PTM-bearing amino acid, Fmoc-Glu(Arg(Pbf)-O^{t}Bu)-OH and incorporated it into peptides for NCL. The arginylated glutamate allowed for facile incorporation into peptides at 37 °C, despite the fact that Fmoc-Arg(Pbf)-OH is known to be difficult to incorporate due to its sterically hindered protected side-chain. In our case, the protected arginine is found at the end of the extended glutamate chain, attached through a peptide bond, making this PTM-bearing amino acid relatively sterically unhindered. Alternative strategies, such as incorporating Alloc-protected Glu and attaching Arg on resin, are also being investigated.

In generating the fragments of αS for the synthesis of full-length arginylated protein, we uncovered some unexpected effects of the copper sulfate/THPTA/sodium ascorbate catalytic system used in click reactions. We noticed that the copper was able to deprotect N-terminal thiazolidines derived from acetaldehyde and formaldehyde, consistent with previously published results,[24] but not thiazolidines derived from pyruvate. This selective reactivity may be due to steric or electronic effects of the carboxylate group on copper coordination to the cysteine sulfur. We also observed, in contrast to the previous report,[24] that the copper led to oxidation of unprotected N-terminal cysteine but that this side reaction could be reduced by argon sparging. Our method for simultaneously deprotecting an N-terminal thiazolidine and labeling an alkynyl amino acid with a fluorophore-azide, used in the synthesis of αS_{56-140}-$C_{56}\pi^{488}{}_{114}$ (**S11**) and αS_{91-140}-$C_{91}\pi^{488}{}_{114}$ (**9**), may be of great utility to future semisynthetic endeavors.

In the semisynthesis of full-length arginylated αS, we explored different synthetic schemes for an N-to-C three-part ligation and investigated the reactivity of MPAA and MTG thiol additives. We developed a novel ligation strategy that involves conversion of the ligation intermediate into a stable MES thioester in order to generate an MTG-thioester *in situ* for reaction with the C-terminal fragment in the second ligation. The higher pK_a and lesser oxidation potential of MTG are likely responsible for its inability to quench excess $NaNO_2$ and therefore prevent it from being a substitute for MPAA during *in situ* conversion of the peptide acyl hydrazide to thioester in a ligation reaction. In standard NCL reactions using MPAA as a thiol additive, following the acyl hydrazide to azide conversion by $NaNO_2$, the MPAA that is added in excess not only allows for thioester formation but also quenches any remaining $NaNO_2$ so that it does not oxidize the ligation handle of the partner peptide.[35] The thiol additive likely eliminates the nitrosonium ion generated *in situ* from $NaNO_2$ through nucleophilic addition. In our reactions, considering the higher pK_a of MTG (pK_a = 7.9) versus that of MPAA (pK_a = 6.6), we reasoned that the MTG was not an effective quencher of $NaNO_2$ compared to MPAA, which, being present predominantly as a thiolate, acts as a better nucleophile. We also cannot exclude the possibility that some of the adducts were due to reactive oxygen species generated *in situ* by NO^+ during the diazotization reaction. Owing to its greater oxidation potential as an aryl thiol, MPAA is known to be a radical quencher,[36] which may serve to protect the N-terminal cysteine of the partner fragment. Other strategies have been developed that employ milder conditions for thioester generation from acyl hydrazide peptides, for example, via acyl pyrazoles, but this weakly activated species requires MPAA for efficient exchange and is therefore incompatible with radical desulfurization.[37] However, our intermediate conversion MTG-thioester generation strategy that allowed for desulfurization without intermediate purification, and thus, the ability to eliminate a lyophilization step, is especially useful for the synthesis of aggregation-prone proteins.

Current semisynthetic methods for the incorporation of a single PTM into αS largely involve deconstructing the protein into two or three fragments.[13] When the modification of interest is found near the terminus, it is possible to semisynthesize the site-specifically modified αS using two fragments such as a recombinant N-terminal fragment and a synthetic C-terminal peptide for phosphorylated Y125[9] or S129.[12] For modification sites farther away from the termini, three-piece ligations have been successfully demonstrated for αS, including that phosphorylated at Y39,[11] nitrated at Y39,[38] or glycosylated at a variety of Ser or Thr sites.[14] These semisyntheses commonly use an N-terminal fragment prepared either by expression in *E. coli* or by SPPS, a synthetic middle fragment bearing the PTM, and an expressed C-terminal fragment. One advantage of the middle fragment being synthetic is that it is possible to carry out a one-pot C-to-N ligation by methoxyamine-mediated activation of the thiazolidine-protected ligation intermediate, although the deprotection takes several hours and necessitates a lowering of pH in addition to requiring purification and lyophilization of the full-length αS before desulfurization. Our N-to-C semisynthesis for singly arginylated αS, with its MES-activated intermediate, MTG-thioester formation, and *in situ* desulfurization, offers a way to overcome these issues.

Alongside the semisynthesis of singly arginylated αS, we established a method to synthesize αS bearing double arginylation and optionally a fluorophore, for a total of three modifications. A number of previous semisyntheses have successfully introduced multiple modifications in αS. Provided that the sites of interest are in proximity, a synthetic middle fragment in a three-piece NCL allows for incorporation of multiple PTMs, as has been shown for αS triply glycosylated at T72/T75/T81.[14] For certain enzymatic PTMs, the strategy of chemoenzymatic semisynthesis, involving the ligation between two recombinant fragments of αS, allows for orthogonal incorporation of multiple modifications: not only PTMs but also fluorophores by thiol-maleimide conjugation and click chemistry.[16] Some other PTMs that are originally enzymatic can be closely mimicked through attachment aided by a small molecule: disulfide-directed ubiquitination[15] or SUMOylation[10] using αS with a cysteine mutation at the site of interest is also compatible with incorporation of modifications at more than one site. In our study, access to triply modified αS having two PTMs and a fluorophore, with each site being in a different region of the protein, is enabled by the C-to-N multipart ligation. Our strategy takes advantage of previously established one-pot ligation methods but optimizes them by maximizing recovery of product when the target protein is aggregation-prone. We synthesized a new ligation handle Alloc-Pen(Trt)-OH and optimized its incorporation into peptides, expanding the toolbox of protected thiol-bearing amino acids for NCL. While Fmoc-protected Pen usage in

https://dx.doi.org/10.1021/jacs.0c10054
J. Am. Chem. Soc. 2020, 142, 21786−21798

ligation is relatively common, the Alloc-protected version permitted the use of Pd-catalyzed *in situ* deprotection, which proceeds to completion in a few minutes. In using Alloc-Pen, we uncovered an unexpected thiol−metal interaction in the form of Pd-TCEP with N-terminal penicillamine, which was absent for the N-terminal cysteine peptides, suggestive of a rigidifying effect exerted by the two methyl groups unique to penicillamine. We found that the use of free H-Pen-OH to strip the Pd allowed this method to be used effectively, but additional investigation could further improve it, and the Pd adduct may serve as an orthogonal N-terminal protecting group. Overall, the strategies that we developed in the semisynthesis of doubly arginylated αS demonstrate a streamlined way to synthesize proteins bearing multiple PTMs and/or fluorophores.

When we investigated the biological effects of arginylation, we found that the modified αS showed no difference in affinity for lipid vesicles compared to WT control. The first ∼30 residues in αS are known to contribute, to various extents, to the energetics of binding to large lipid vesicles,[39] where αS adopts an extended helix. A model has also been proposed in which the first ∼90 residue segment of lipid-bound αS displays two α11/3 helical regions with a single break, resulting in an amphipathic structure with well-defined hydrophobic and hydrophilic faces.[40] While the glutamate side chain is negatively charged and the arginine side chain is positively charged at physiological pH, the arginylated glutamate is zwitterionic (Figure 1). Obviously, the arginylated glutamate is also much larger than any canonical amino acid. The fact that arginylation at either glutamate 46 or 83 or both had no impact on the affinity of αS to lipid vesicles implies that these residues may not contribute significantly to lipid binding. The E^{Arg}_{46} result is consistent with the α11/3 helix model that places E_{46} facing away from the lipid membrane but is in contrast to results showing that the disease mutation $E_{46}K$ enhances the binding of αS to lipid vesicles.[33,34] Our results show that the precise chemical nature of the PTM must be taken into account and caution one against drawing conclusions regarding PTMs from corresponding mutations to canonical amino acids.

Finally, when investigating the effect of arginylation on αS aggregation, we identified a protective effect of this PTM against fibril formation, slowing kinetics and reducing monomer incorporation into fibrils. Arginylation at E_{83} slowed aggregation, and double arginylation displayed protective effects that were more significant than would be predicted by a simple combination of each individual arginylation effect. The fact that arginylation of E_{46} alone did not contribute to deceleration of fibril formation or monomer incorporation is somewhat surprising, as E_{46} forms a salt bridge with K_{80} in most polymorphs of WT αS fibrils,[41] and the switch from the negatively charged glutamate to the net neutral E^{Arg} would be expected to destabilize such an interaction. The mutation $E_{46}K$ is implicated in Parkinson's disease[8,42] and is known to disrupt fibril formation,[43] but E^{Arg}_{46} does not seem to interfere with this process. The significant effect that arginylation at E_{83} displays in reducing monomer incorporation into fibrils may be due to the fact that it is immediately adjacent in sequence to the innermost β-sheet of the core (residues 71−82) in the "Greek key" motif of αS fibrils, which is established by a hydrophobic pocket.[41] The fibril-destabilizing effect of arginylation at site 83 and the combined effect of arginylation at both sites corroborate the purported neuroprotective role for arginylation in Parkinson's disease. It is interesting that doubly arginylated αS dramatically slows aggregation but does not alter monomer incorporation to a greater degree than a single E^{Arg}_{83} modification, implying a complex interplay of kinetic and thermodynamic effects on fibril formation.

CONCLUSION

In this study, we integrated a multitude of techniques to access arginylated αS and identified the effect of this PTM on the protein's native role and behavior in disease. By assaying its aggregation, we determined that arginylated αS displays neuroprotective effects, slowing the formation of fibrils and reducing monomer incorporation. Through biophysical characterizations of the interaction between arginylated αS and lipid vesicles, we determined that the PTM does not alter the native role of αS. In the case of an understudied PTM such as arginylation, semisynthesis of the modified protein is invaluable, as it allows site-specific installation of the modification. Synthesis of the novel arginylated glutamate amino acid allowed us to study the authentic PTM, offering an advantage over site-directed mutagenesis to a natural amino acid mimic, as these often do not recapitulate the effects of the authentic modification. By optimizing the incorporation of arginylation by SPPS and NCL, we developed methods more straightforward than the laborious screening process needed to evolve a tRNA/synthetase pair that would recognize and incorporate E^{Arg} recombinantly and at more than one site. Our ligation strategies for both singly and doubly arginylated aS are also amenable to the installation of fluorophores, which are indispensable in biophysical studies that characterize the behavior of biologically relevant macromolecules. The Alloc-penicillamine that we synthesized adds another ligation handle to the NCL toolbox and expands the possible sites of one-pot ligation from native alanines to also include native valines. The synthesis of an unusual PTM-bearing amino acid, incorporation of a novel ligation handle by SPPS and NCL, and semisynthetic methods for multiply modified αS that we have developed here pave the way for further investigation of complex PTMs and their cooperative effects in disordered proteins and beyond.

ASSOCIATED CONTENT

Supporting Information

The Supporting Information is available free of charge at https://pubs.acs.org/doi/10.1021/jacs.0c10054.

Detailed procedures for peptide synthesis, protein expression, ligation procedures and purification, as well as aggregation and FCS data (PDF)

AUTHOR INFORMATION

Corresponding Authors

Elizabeth Rhoades − *Department of Chemistry, University of Pennsylvania, Philadelphia, Pennsylvania 19104, United States*; Email: elizabeth.rhoades@sas.upenn.edu

E. James Petersson − *Department of Chemistry, University of Pennsylvania, Philadelphia, Pennsylvania 19104, United States*; orcid.org/0000-0003-3854-9210; Email: ejpetersson@sas.upenn.edu

Authors

Buyan Pan − *Department of Chemistry, University of Pennsylvania, Philadelphia, Pennsylvania 19104, United States*

https://dx.doi.org/10.1021/jacs.0c10054
J. Am. Chem. Soc. 2020, 142, 21786−21798

Naoki Kamo − *Department of Chemistry, University of Pennsylvania, Philadelphia, Pennsylvania 19104, United States; Department of Chemistry and Biotechnology, Graduate School of Engineering, The University of Tokyo, Tokyo 113-8656, Japan*

Marie Shimogawa − *Department of Chemistry, University of Pennsylvania, Philadelphia, Pennsylvania 19104, United States*

Yun Huang − *Department of Chemistry, University of Pennsylvania, Philadelphia, Pennsylvania 19104, United States*

Anna Kashina − *Department of Biomedical Sciences, University of Pennsylvania School of Veterinary Medicine, Philadelphia, Pennsylvania 19104, United States*

Complete contact information is available at: https://pubs.acs.org/10.1021/jacs.0c10054

Notes

The authors declare no competing financial interest.

■ ACKNOWLEDGMENTS

This research was supported by the National Institutes of Health (NIH Grant NS103873 to E.J.P., Grant NS102435 to A.K. and E.J.P., and Grant NS079955 to E.R.). Instruments supported by the NIH and the NSF include NMR (NSF Grant CHE-1827457), HRMS (NIH Grant RR-023444), and MALDI-MS (NSF Grant MRI-0820996). B.P. thanks the University of Pennsylvania for support through a Dissertation Completion Fellowship. N.K. thanks the Japan Society for Promotion of Science (JSPS) Overseas Challenge Program for Young Researchers for funding. M.S. thanks the Nakajima Foundation for scholarship funding.

■ REFERENCES

(1) Spillantini, M. G.; Schmidt, M. L.; Lee, V. M. Y.; Trojanowski, J. Q.; Jakes, R.; Goedert, M. Alpha-Synuclein in Lewy Bodies. *Nature* **1997**, *388*, 839−840.

(2) Wang, J. L.; Han, X. M.; Saha, S.; Xu, T.; Rai, R.; Zhang, F. L.; Wolf, Y. I.; Wolfson, A.; Yates, J. R.; Kashina, A. Arginyltransferase Is an Atp-Independent Self-Regulating Enzyme That Forms Distinct Functional Complexes in Vivo. *Chem. Biol.* **2011**, *18*, 121−130.

(3) Wong, C. C. L.; Xu, T.; Rai, R.; Bailey, A. O.; Yates, J. R.; Wolf, Y. I.; Zebroski, H.; Kashina, A. Global Analysis of Posttranslational Protein Arginylation. *PLoS Biol.* **2007**, *5*, 2231−2242.

(4) Xu, T.; Wong, C. C. L.; Kashina, A.; Yates, J. R. Identification of N-Terminally Arginylated Proteins and Peptides by Mass Spectrometry. *Nat. Protoc.* **2009**, *4*, 325−332.

(5) Wang, J. L.; Han, X. M.; Wong, C. C. L.; Cheng, H.; Aslanian, A.; Xu, T.; Leavis, P.; Roder, H.; Hedstrom, L.; Yates, J. R.; et al. Arginyltransferase Ate1 Catalyzes Midchain Arginylation of Proteins at Side Chain Carboxylates in Vivo. *Chem. Biol.* **2014**, *21*, 331−337.

(6) Wang, J. L.; Han, X. M.; Leu, N. A.; Sterling, S.; Kurosaka, S.; Fina, M.; Lee, V. M.; Dong, D. W.; Yates, J. R.; Kashina, A. Protein Arginylation Targets Alpha Synuclein, Facilitates Normal Brain Health, and Prevents Neurodegeneration. *Sci. Rep.* **2017**, *7*, 14.

(7) Greenbaum, E. A.; Graves, C. L.; Mishizen-Eberz, A. J.; Lupoli, M. A.; Lynch, D. R.; Englander, S. W.; Axelsen, P. H.; Giasson, B. I. The E46k Mutation in Alpha-Synuclein Increases Amyloid Fibril Formation. *J. Biol. Chem.* **2005**, *280*, 7800−7807.

(8) Zarranz, J. J.; Alegre, J.; Gomez-Esteban, J. C.; Lezcano, E.; Ros, R.; Ampuero, I.; Vidal, L.; Hoenicka, J.; Rodriguez, O.; Atares, B.; et al. The New Mutation, E46k, of Alpha-Synuclein Causes Parkinson and Lewy Body Dementia. *Ann. Neurol.* **2004**, *55*, 164−173.

(9) Hejjaoui, M.; Butterfield, S.; Fauvet, B.; Vercruysse, F.; Cui, J.; Dikiy, I.; Prudent, M.; Olschewski, D.; Zhang, Y.; Eliezer, D.; et al. Elucidating the Role of C-Terminal Post-Translational Modifications Using Protein Semisynthesis Strategies: Alpha-Synuclein Phosphorylation at Tyrosine 125. *J. Am. Chem. Soc.* **2012**, *134*, 5196−5210.

(10) Abeywardana, T.; Pratt, M. R. Extent of Inhibition of Alpha-Synuclein Aggregation in Vitro by Sumoylation Is Conjugation Site- and Sumo Isoform-Selective. *Biochemistry* **2015**, *54*, 959−961.

(11) Dikiy, I.; Fauvet, B.; Jovicic, A.; Mahul-Mellier, A. L.; Desobry, C.; El-Turk, F.; Gitler, A. D.; Lashuel, H. A.; Eliezer, D. Semisynthetic and in Vitro Phosphorylation of Alpha-Synuclein at Y39 Promotes Functional Partly Helical Membrane-Bound States Resembling Those Induced by Pd Mutations. *ACS Chem. Biol.* **2016**, *11*, 2428−2437.

(12) Ma, M. R.; Hu, Z. W.; Zhao, Y. F.; Chen, Y. X.; Li, Y. M. Phosphorylation Induces Distinct Alpha-Synuclein Strain Formation. *Sci. Rep.* **2016**, *6*, 11.

(13) Chen, H.; Zhao, Y. F.; Chen, Y. X.; Li, Y. M. Exploring the Roles of Post-Translational Modifications in the Pathogenesis of Parkinson's Disease Using Synthetic and Semisynthetic Modified Alpha-Synuclein. *ACS Chem. Neurosci.* **2019**, *10*, 910−921.

(14) Levine, P. M.; Galesic, A.; Balana, A. T.; Mahul-Mellier, A. L.; Navarro, M. X.; De Leon, C. A.; Lashuel, H. A.; Pratt, M. R. Alpha-Synuclein O-Glcnacylation Alters Aggregation and Toxicity, Revealing Certain Residues as Potential Inhibitors of Parkinson's Disease. *Proc. Natl. Acad. Sci. U. S. A.* **2019**, *116*, 1511−1519.

(15) Moon, S. P.; Balana, A. T.; Galesic, A.; Rakshit, A.; Pratt, M. R. Ubiquitination Can Change the Structure of the Alpha-Synuclein Amyloid Fiber in a Site Selective Fashion. *J. Org. Chem.* **2020**, *85*, 1548−1555.

(16) Pan, Y.; Rhoades, E.; Petersson, E. J. Chemoenzymatic Semisynthesis of Phosphorylated Alpha-Synuclein Enables Identification of a Bidirectional Effect on Fibril Formation. *ACS Chem. Biol.* **2020**, *15*, 640−645.

(17) Wissner, R. F.; Wagner, A. M.; Warner, J. B.; Petersson, E. J. Efficient, Traceless Semi-Synthesis of A-Synuclein Labeled with a FluoroPhore/Thioamide Fret Pair. *Synlett* **2013**, *24*, 2454−2458.

(18) Tanaka, T.; Wagner, A. M.; Warner, J. B.; Wang, Y. J.; Petersson, E. J. Expressed Protein Ligation at Methionine: N-Terminal Attachment of Homocysteine, Ligation, and Masking. *Angew. Chem., Int. Ed.* **2013**, *52*, 6210−6213.

(19) Batjargal, S.; Wang, Y. J.; Goldberg, J. M.; Wissner, R. F.; Petersson, E. J. Native Chemical Ligation of Thioamide-Containing Peptides: Development and Application to the Synthesis of Labeled α-Synuclein for Misfolding Studies. *J. Am. Chem. Soc.* **2012**, *134*, 9172−9182.

(20) Haase, C.; Rohde, H.; Seitz, O. Native Chemical Ligation at Valine. *Angew. Chem., Int. Ed.* **2008**, *47*, 6807−6810.

(21) Haney, C. M.; Wissner, R. F.; Warner, J. B.; Wang, Y. X. J.; Ferrie, J. J.; Covell, D. J.; Karpowicz, R. J.; Lee, V. M. Y.; Petersson, E. J. Comparison of Strategies for Non-Perturbing Labeling of Alpha-Synuclein to Study Amyloidogenesis. *Org. Biomol. Chem.* **2016**, *14*, 1584−1592.

(22) Rostovtsev, V. V.; Green, L. G.; Fokin, V. V.; Sharpless, K. B. A Stepwise Huisgen Cycloaddition Process: Copper(I)-Catalyzed Regioselective "Ligation" of Azides and Terminal Alkynes. *Angew. Chem., Int. Ed.* **2002**, *41*, 2596−2599.

(23) Hong, V.; Presolski, S. I.; Ma, C.; Finn, M. G. Analysis and Optimization of Copper-Catalyzed Azide-Alkyne Cycloaddition for Bioconjugation. *Angew. Chem., Int. Ed.* **2009**, *48*, 9879−9883.

(24) Naruse, N.; Kobayashi, D.; Ohkawachi, K.; Shigenaga, A.; Otaka, A. Copper-Mediated Deprotection of Thiazolidine and Selenazolidine Derivatives Applied to Native Chemical Ligation. *J. Org. Chem.* **2020**, *85*, 1425−1433.

(25) Zhao, Z. G.; Metanis, N. Copper-Mediated Selenazolidine Deprotection Enables One-Pot Chemical Synthesis of Challenging Proteins. *Angew. Chem., Int. Ed.* **2019**, *58*, 14610−14614.

(26) Lee, D. J.; Mandal, K.; Harris, P. W. R.; Brimble, M. A.; Kent, S. B. H. A One-Pot Approach to Neoglycopeptides Using Orthogonal Native Chemical Ligation and Click Chemistry. *Org. Lett.* **2009**, *11*, 5270−5273.

(27) Huang, Y. C.; Chen, C. C.; Gao, S.; Wang, Y. H.; Xiao, H.; Wang, F.; Tian, C. L.; Li, Y. M. Synthesis of L- and D-Ubiquitin by One-Pot Ligation and Metal-Free Desulfurization. *Chem. - Eur. J.* **2016**, *22*, 7623−7628.
(28) Kamo, N.; Hayashi, G.; Okamoto, A. Triple Function of 4-Mercaptophenylacetic Acid Promotes One-Pot Multiple Peptide Ligation. *Angew. Chem., Int. Ed.* **2018**, *57*, 16533−16537.
(29) El-Agnaf, O. M. A.; Bodles, A. M.; Guthrie, D. J. S.; Harriott, P.; Irvine, G. B. The N-Terminal Region of Non-a Beta Component of Alzheimer's Disease Amyloid Is Responsible for Its Tendency to Assume Beta-Sheet and Aggregate to Form Fibrils. *Eur. J. Biochem.* **1998**, *258*, 157−163.
(30) Beesley, R. M.; Ingold, C. K.; Thorpe, J. F. The Formation and Stability of Spiro-Compounds. *J. Chem. Soc., Trans.* **1915**, *107*, 1080−1106.
(31) Allinger, N. L.; Zalkow, V. Conformational Analysis 0.9. The Gem-Dimethyl Effect. *J. Org. Chem.* **1960**, *25*, 701−704.
(32) Middleton, E. R.; Rhoades, E. Effects of Curvature and Composition on Alpha-Synuclein Binding to Lipid Vesicles. *Biophys. J.* **2010**, *99*, 2279−2288.
(33) Bodner, C. R.; Maltsev, A. S.; Dobson, C. M.; Bax, A. Differential Phospholipid Binding of Alpha-Synuclein Variants Implicated in Parkinson's Disease Revealed by Solution Nmr Spectroscopy. *Biochemistry* **2010**, *49*, 862−871.
(34) Stockl, M.; Fischer, P.; Wanker, E.; Herrmann, A. Alpha-Synuclein Selectively Binds to Anionic Phospholipids Embedded in Liquid-Disordered Domains. *J. Mol. Biol.* **2008**, *375*, 1394−1404.
(35) Zheng, J. S.; Tang, S.; Qi, Y. K.; Wang, Z. P.; Liu, L. Chemical Synthesis of Proteins Using Peptide Hydrazides as Thioester Surrogates. *Nat. Protoc.* **2013**, *8*, 2483−2495.
(36) Rohde, H.; Schmalisch, J.; Harpaz, Z.; Diezmann, F.; Seitz, O. Ascorbate as an Alternative to Thiol Additives in Native Chemical Ligation. *ChemBioChem* **2011**, *12*, 1396−1400.
(37) Flood, D. T.; Hintzen, J. C. J.; Bird, M. J.; Cistrone, P. A.; Chen, J. S.; Dawson, P. E. Leveraging the Knorr Pyrazole Synthesis for the Facile Generation of Thioester Surrogates for Use in Native Chemical Ligation. *Angew. Chem., Int. Ed.* **2018**, *57*, 11634−11639.
(38) Burai, R.; Ait-Bouziad, N.; Chiki, A.; Lashuel, H. A. Elucidating the Role of Site-Specific Nitration of Alpha-Synuclein in the Pathogenesis of Parkinson's Disease Via Protein Semisynthesis and Mutagenesis. *J. Am. Chem. Soc.* **2015**, *137*, 5041−5052.
(39) Fusco, G.; De Simone, A.; Arosio, P.; Vendruscolo, M.; Veglia, G.; Dobson, C. M. Structural Ensembles of Membrane-Bound Alpha-Synuclein Reveal the Molecular Determinants of Synaptic Vesicle Affinity. *Sci. Rep.* **2016**, *6*, 9.
(40) Bussell, R.; Eliezer, D. A Structural and Functional Role for 11-Mer Repeats in Alpha-Synuclein and Other Exchangeable Lipid Binding Proteins. *J. Mol. Biol.* **2003**, *329*, 763−778.
(41) Tuttle, M. D.; Comellas, G.; Nieuwkoop, A. J.; Covell, D. J.; Berthold, D. A.; Kloepper, K. D.; Courtney, J. M.; Kim, J. K.; Barclay, A. M.; Kendall, A.; et al. Solid-State Nmr Structure of a Pathogenic Fibril of Full-Length Human Alpha-Synuclein. *Nat. Struct. Mol. Biol.* **2016**, *23*, 409−415.
(42) Polymeropoulos, M. H.; Lavedan, C.; Leroy, E.; Ide, S. E.; Dehejia, A.; Dutra, A.; Pike, B.; Root, H.; Rubenstein, J.; Boyer, R.; et al. Mutation in the Alpha-Synuclein Gene Identified in Families with Parkinson's Disease. *Science* **1997**, *276*, 2045−2047.
(43) Li, Y. W.; Zhao, C. Y.; Luo, F.; Liu, Z. Y.; Gui, X. R.; Luo, Z. P.; Zhang, X.; Li, D.; Liu, C.; Li, X. M. Amyloid Fibril Structure of Alpha-Synuclein Determined by Cryoelectron Microscopy. *Cell Res.* **2018**, *28*, 897−903.

https://dx.doi.org/10.1021/jacs.0c10054
J. Am. Chem. Soc. 2020, 142, 21786−21798